

Myocardial ischemia testing with computed tomography: emerging strategies

Prabhakar Rajiah¹, Christopher D. Maroules²

¹Department of Radiology, Cardiothoracic Imaging, UT Southwestern Medical Center, Dallas, Texas, USA; ²Department of Radiology, Naval Medical Center, Portsmouth, Virginia, USA

Contributions: (I) Conception and design: P Rajiah; (II) Administrative support: P Rajiah; (III) Provision of study material or patients: P Rajiah; (IV) Collection and assembly of data: All authors; (V) Data analysis and interpretation: All authors; (VI) Manuscript writing: All authors; (VII) Final approval of manuscript: All authors.

Correspondence to: Prabhakar Rajiah, MBSS, MD, FRCR. Associate Professor, Department of Radiology, Cardiothoracic Imaging, UT Southwestern Medical Center, E6.120 B, Mail Code 9316, 5323 Harry Hines Boulevard, Dallas, TX 75390-8896, USA. Email: radprabhakar@gmail.com.

Abstract: Although cardiac computed tomography (CT) has high negative predictive value to exclude obstructive coronary artery disease (CAD), particularly in the low to intermediate risk population, it has low specificity in the diagnosis of ischemia-inducing lesions. This inability to predict hemodynamically significant stenosis hampers the ability of CT to be an effective gatekeeper for invasive angiography and to guide appropriate revascularization. Recent advances in CT technology have resulted in the development of multiple techniques to provide hemodynamic information and detect lesion-specific ischemia, namely CT perfusion (CTP), CT-derived fractional flow reserve (CT-FFR) and coronary transluminal attenuation gradient (TAG). In this article, we provide a perspective on these emerging CT techniques in the evaluation of myocardial ischemia.

Keywords: Cardiac computed tomography (CT); myocardial ischemia; CT perfusion (CTP); flow; CT-derived fractional flow reserve (CT-FFR)

Submitted Jul 19, 2016. Accepted for publication Sep 01, 2017.

doi: 10.21037/cdt.2017.09.06

View this article at: <http://dx.doi.org/10.21037/cdt.2017.09.06>

Introduction

Coronary computed tomography angiogram (CCTA) has high accuracy and negative predictive value (NPV) in the evaluation of coronary artery disease (CAD), particularly in the low to intermediate risk population, both in the stable and emergency settings (1-3). In current practice, CTA is used in symptomatic patients in the low-to-intermediate risk category with equivocal stress tests or those unable to perform stress test; however, it can be used as an index test in these patients since studies have shown similar clinical effectiveness to stress testing (4-8). CCTA also provides information on the vessel wall and characteristics of atherosclerotic plaques. CT is however limited in its ability to characterize the hemodynamic significance of a stenotic lesion, with low specificity (39% per-patient, 58% per-

vessel) and low positive predictive value (PPV) compared to invasive fractional flow reserve (FFR) (9,10). Knowledge of the functional consequence of an intermediate coronary arterial stenosis is required for further management, including the need for further invasive coronary angiogram (ICA), which is typically provided by stress tests such as exercise stress test, stress echocardiogram, stress perfusion magnetic resonance imaging (MRI) and nuclear medicine techniques [single-photon emission CT (SPECT) and positron emission tomography (PET)]. These tests are not perfect and hence up to 63% of ICA studies end up being unnecessary, with either normal or non-obstructive CAD, in spite of a majority of these patients (up to 84%) having had a prior positive non-invasive imaging test (11,12). Accurate functional information is provided by invasive

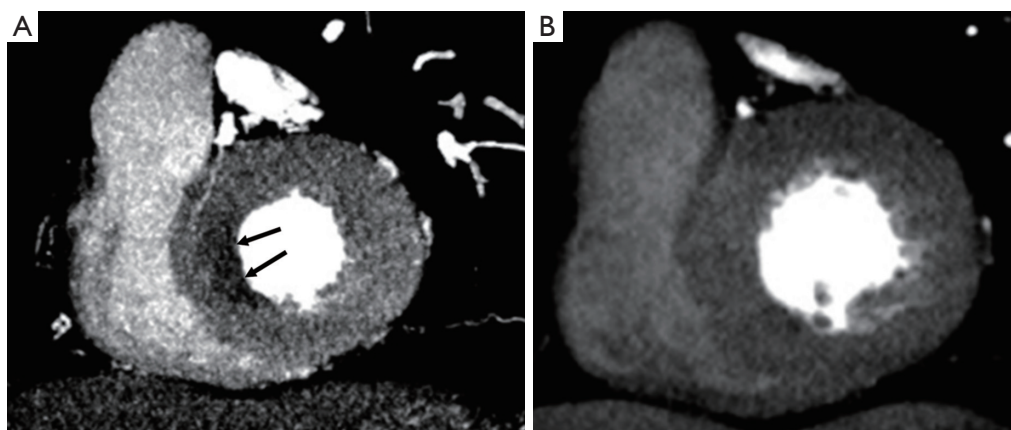


Figure 1 CT perfusion. (A) Short axis stress perfusion CT image obtained at 45% of R-R interval in a patient with chest pain, shows a sub-endocardial perfusion defect in the basal septum (arrows); (B) rest CT perfusion image in the same patient at the same level does not show the defect. These findings are consistent with reversible myocardial ischemia. CT, computed tomography.

FFR during the ICA, and FFR-guided revascularization has shown improved outcomes and lower cost compared to angiographic stenosis-guided revascularization (13,14). However, due to the small but finite risks of cardiac catheterization, it is not appropriate to perform invasive FFR in all patients with suspected CAD.

Hence, there is a need for a reliable non-invasive imaging test that can accurately identify lesion-specific ischemia, act as an effective gatekeeper for ICA, reduce unnecessary ICA, and guide appropriate revascularization, all of which will result in improved clinical outcomes and lower costs. Since CT provides good morphological information including the vessel wall, if it is also able to provide functional information, it can potentially become a one-stop shop imaging modality in the evaluation of CAD. Recent advances in CT technology have resulted in the development of multiple techniques to provide hemodynamic information and detect lesion-specific ischemia, namely CT perfusion (CTP), CT-derived FFR (CT-FFR) and coronary transluminal attenuation gradient (TAG). In this article, we provide a perspective on these emerging CT techniques in the evaluation of myocardial ischemia.

CTP

CTP utilizes the iodine uptake of myocardium during the first pass of contrast as a surrogate for myocardial perfusion with ischemia characterized by reversible low myocardial attenuation (hypoperfusion) on stress images, with normal

myocardial attenuation on resting images (*Figure 1*). CTP techniques are heterogeneous, either static or dynamic and can be done with either single or dual energy technology. Single-energy scanners can be conventional, wide-detector array/volume scanners or dual-source with high-pitch helical mode and dual-energy scanners can be dual source, rapid kVp switching or dual layer technology. A variety of pharmacological agents can be used for provocative stress, the most common of which include the coronary vasodilators adenosine and regadenoson. A variety of CTP protocols have been described, with rest and stress images obtained in variable order, with or without delayed enhancement for estimation of myocardial scar/fibrosis. Static CTP provides a snapshot of myocardial perfusion in one timeframe, usually 8–16 seconds after peak aortic attenuation. Although this does not provide quantitative information, qualitative or semi-quantitative (transmural perfusion ratio) measurements can be obtained. Qualitative analysis of ischemia depends on relative myocardial hypoattenuation compared to normal attenuation of the adjacent myocardium. Thus, analogous to SPECT myocardial perfusion imaging (MPI), balanced ischemia of all three myocardial territories may be missed (15,16). Dual energy techniques have improved sensitivity and specificity for detecting myocardial perfusion defects by using virtual monoenergetic images and iodine maps which can reduce beam-hardening artifacts (15) and allow quantification of myocardial blood flow. Beam hardening artifacts are caused by polyenergetic nature of the X-ray beam and lead to low attenuation in the myocardium adjacent to dense

contrast in left ventricular (LV) blood pool, especially in the posterobasal wall, mimicking perfusion defect. Virtual monoenergetic images at higher energies (>70 keV) have been shown to have lower beam hardening (17-20). Dynamic CTP images the myocardium several times during the first pass of contrast and generates a time attenuation curve, from which perfusion can be measured using semi-quantitative or fully automated quantitative techniques. However, dynamic CTP is associated with higher radiation exposure, longer breath-hold time, and spatial misregistration compared to static CTP.

CTP has been validated in multiple trials against SPECT, PET, MRI and ICA (*Table 1*). Single-energy static CTP has overall sensitivity of 50–96%, specificity of 68–98%, NPV of 79–98% and PPV of 55–94% (16). Dual-energy static CTP has overall sensitivity of 68–99%, specificity of 72–99%, NPV of 79–98 % and accuracy of 83–97% (16). In a meta-analysis, combined CTA and CTP showed pooled per-vessel sensitivity and specificity of 85% and 93% respectively for diagnosing >50% stenosis with ICA as the gold standard (53). Against the invasive FFR gold standard, a small study of 42 patients in a 320-slice scanner showed that CTP has 84% specificity and 82% PPV on a per-vessel basis in the diagnosis of lesion specific ischemia (33). The combination >50% stenosis on CTA and perfusion defect on CTP is 98% specific for ischemia, while stenosis <50% and normal perfusion on CTP is 100% specific for excluding ischemia (33). Another meta-analysis with invasive FFR as gold standard found that CTP can exclude hemodynamically significant stenosis and serve as an effective gatekeeper for ICA with a per-patient negative likelihood ratio of 0.12, which is comparable to MRI (0.14) and PET (0.14) and superior to SPECT (0.39) and echo (0.42) (54). Further, in a small study on 48 patients from the CORE320 trial who underwent ICA, CTA and either CTP, MRI or SPECT, patient satisfaction was higher when using a strategy of combined CTA + CTP (55).

Although no large-scale outcomes data exist for CTP, similar data from SPECT-MPI show that MPI can increase continuous net reclassification index (NRI) by 49.4%, reclassifying 66.5% as lower risk and 32.8% at higher risk of death or non-fatal myocardial infarction (MI) (56). A recent study with dynamic CTP showed that the presence and number of perfusion defects were associated with higher risk of major adverse cardiac events (MACE), which is incremental over clinical risk factors and obstructive coronary stenosis in CTA (57). Adding CTP to CTA results in 5-fold reduction in downstream ICA and revascularization with a low 12-month MACE rate (58).

CTP with dual-energy has also shown to be more cost-effective than SPECT, with an incremental cost-effective ratio (ICER) \$3,191 per quality-adjusted life year (QALY) compared to \$3,357 per QALY for SPECT (59).

However, CTP is not widely available in all CT centers, and requires advanced skills in performance, post-processing and interpretation. CTP is also associated with higher radiation exposure, larger volume of iodine contrast and higher costs when compared to CTA alone. Radiation exposure estimates range from 4.5 to 9 mSv for static CTP techniques, which remain lower than traditional SPECT MPI protocols (60).

CT-FFR

CT-FFR is a non-invasive technique of estimating FFR across a coronary stenosis using anatomic data from cardiac CT without any protocol change or additional contrast/radiation. It is based on computational fluid dynamics modelling of cardiac CT data using advanced post-processing and 3D Navier-Stokes equations to solve for flow and pressure measurements across the coronary vascular bed. Currently, CT-FFR relies on a series of mathematical assumptions including the relationship between resting myocardial blood flow and mass, the relationship between microvascular resistance and epicardial coronary size, and a predictable coronary response to adenosine. Such assumptions may limit the accuracy of CT-FFR in certain patient populations (e.g., unstable angina). Hyperemic state is simulated by reducing microvascular resistance by a factor of 0.21. Currently, the most commonly used platform is the *HeartFlow*, in which data is transferred off-site for advanced post-processing, although there are on-site vendor-based hybrid platforms (e.g., Siemens) which use machine learning, reduced-order models in non-stenotic regions and pressure drop models in stenotic regions (61,62). CT-FFR <0.8 is used as a cut-off for a functionally significant stenosis (*Figure 2*). In many centers, CT-FFR data is usually requested retrospectively if moderate luminal stenosis is detected on CTA, to evaluate if the lesion is hemodynamically significant. Interestingly, FFR has been shown to be abnormal in 16.6% of patients with <50% stenosis [ischemia without stenosis (IWOS)], normal in 33% of patients with >70% stenosis [stenosis without ischemia (SWOI)] and abnormal in only 50% of patients with moderate (50–70%) stenosis, suggesting CT-FFR may be appropriate for interrogating a wider spectrum of coronary lesions (63,64). In the case of tandem

Table 1 Diagnostic performance of CT perfusion in various studies

Studies	Acquisition	Energy	Reference standard	Level	Sensitivity (%)	Specificity (%)	PPV (%)	NPV (%)
Kurata <i>et al.</i> (21)	Static	Single	ICA	Vessel	90	79	NA	NA
George <i>et al.</i> (22)	Static	Single	SPECT	Vessel	50	89	55	87
Blankstein <i>et al.</i> (23)	Static	Single	SPECT	Vessel	84	80	71	90
Cury (24)	Static	Single	SPECT	Patient	94	78	89	87
George <i>et al.</i> (25)	Static	Single	SPECT, ICA	Patient	86	92	92	85
Cury <i>et al.</i> (26)	Static	Single	SPECT, ICA	Vessel	88	79	67	93
Rochitte <i>et al.</i> (27)	Static	Single	SPECT, ICA	Patient	80	74	65	86
Nasis <i>et al.</i> (28)	Static	Single	SPECT, ICA	Vessel	94	98	94	98
Osawa <i>et al.</i> (29)	Static	Single	ICA	Vessel	85	94	79	96
Kachenoura <i>et al.</i> (30)	Static	Single	ICA	Patient	96	68	88	87
Rocha-Filho <i>et al.</i> (31)	Static	Single	ICA	Vessel	91	91	86	83
Bettencourt <i>et al.</i> (32)	Static	Single	Invasive FFR	Patient	89	83	80	90
Ko <i>et al.</i> (33)	Static	Single	Invasive FFR	Vessel	76	84	82	79
Feuchtner <i>et al.</i> (34)	Static	Single	MRI	Vessel	96	88	93	94
Weininger <i>et al.</i> (35)	Dynamic	Single	SPECT	Segment	84	92	88	92
	Dynamic	Single	MRI	Segment	86	98	94	96
Ho <i>et al.</i> (36)	Dynamic	Single	SPECT, ICA	Segment	83	78	79	82
Wang <i>et al.</i> (37)	Dynamic	Single	SPECT, ICA	Segment	85	92	55	98
Greif <i>et al.</i> (38)	Dynamic	Single	Invasive FFR	Vessel	95	74	48	98
Rossi <i>et al.</i> (39)	Dynamic	Single	Invasive FFR	Vessel	88	90	77	95
Huber <i>et al.</i> (40)	Dynamic	Single	Invasive FFR	Vessel	76	100	100	90
Bamberg <i>et al.</i> (41)	Dynamic	Single	Invasive FFR	Vessel	93	87	75	97
	Dynamic	Single	MRI	Vessel	100	75	92	100
Bastarrika <i>et al.</i> (42)	Dynamic	Single	MRI	Segment	86	98	94	96
Meinel <i>et al.</i> (43)	Static	Dual	SPECT	Segment	99	97	92	100
Ruzsics <i>et al.</i> (44)	Static	Dual	SPECT	Segment	92	93	83	97
Carrascosa <i>et al.</i> (45)	Static	Dual	SPECT	Segment	74	95	–	–
Kido <i>et al.</i> (46)	Static	Dual	ICA	Vessel (CTP + CTA)	67	92	84	82
De Cecco <i>et al.</i> (47)	Static	Dual	ICA, SPECT	Patient	95	50	NA	NA
Wang <i>et al.</i> (48)	Static	Dual	SPECT, ICA	Segment	89	98	87	98
Ko <i>et al.</i> (49)	Static	Dual	ICA	Vessel	89	74	80	85
Ko <i>et al.</i> (50)	Static	Dual	MRI, ICA	Vessel	42	83	59	70
Kim <i>et al.</i> (51)	Static	Dual	MRI	Segment	77	94	53	98
Ko <i>et al.</i> (52)	Static	Dual	MRI	Segment	89	78	74	91

PPV, positive predictive value; NPV, negative predictive value; ICA, invasive coronary angiogram; SPECT, single-photon emission computed tomography; FFR, fractional flow reserve; MRI, magnetic resonance imaging; CTA, computed tomography angiogram; CTP, CT perfusion; NA, not available.

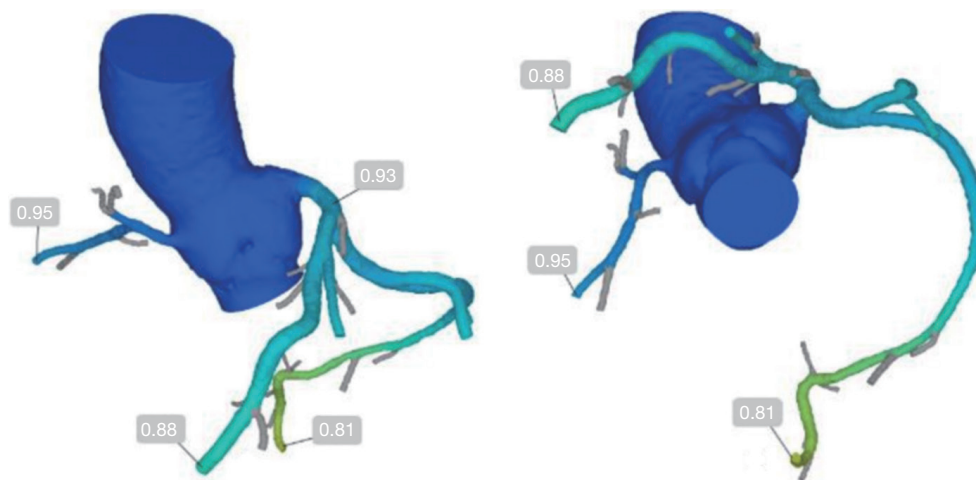


Figure 2 CT fractional flow reserve. CT-FFR values from a patient with acute chest pain and intermediate coronary artery stenosis in CTA were above 0.8, indicating that there is no hemodynamically significant coronary arterial narrowing. CT-FFR, computed tomography-derived fractional flow reserve; CTA, computed tomography angiogram.

lesions, CT-FFR has been shown to guide revascularization by identifying hemodynamically-significant culprit lesion(s) and predict the response to revascularization by placing a virtual stent (65).

Several studies have been performed using CT-FFR with good accuracy (Table 2) (61,62,66-72). Trials such as DISCOVER-FLOW, DEFACTO and NXT performed with the HeartFlow platform have shown significantly improved specificity of CT-FFR compared to conventional CTA (82% *vs.* 25%, 54% *vs.* 42%, 79% *vs.* 34%, respectively) for lesion-specific ischemia using invasive FFR as the gold standard, without compromising sensitivity on a per-patient basis (66-68). Studies performed with on-site platforms have also shown improved specificity of CT-FFR over CTA alone (85% *vs.* 32% and 65% *vs.* 38%) (69). A meta-analysis of five studies showed that on a per-patient basis, the pooled specificity of CT-FFR is 70% compared to 35% for conventional CTA, with additional improvements in accuracy (83% *vs.* 55%), PPV (69% *vs.* 51%), NPV (90% *vs.* 83%), and area under the curve (AUC) (0.87 *vs.* 0.74), and comparable sensitivity (89% *vs.* 90%) (71). A meta-analysis of all the seven studies showed pooled estimates of sensitivity, specificity and diagnostic odds ratio for detection of ischemic lesions of 0.89, 0.76 and 26.2, respectively (72). Another meta-analysis of all imaging methods with invasive-FFR as gold standard showed a sensitivity of 90% and specificity of 71% for CT-FFR, compared to 90% and 39% respectively for CTA, with improved specificity generated

by coupling CTA and CT-FFR (10).

The improved specificity of CT-FFR beyond CTA results in conversion of false-positives to true-negatives (68% reclassification in NXT trial) in the intermediate risk group in CTA, which significantly decreases the rate of non-obstructive disease in ICA, thus improving the capabilities of CT as a gatekeeper for ICA, and selecting optimal patients for revascularization. In the RIPCORD study on 200 patients of the NXT trial, interventional cardiologists were asked to make a consensus decision on management [medical *vs.* percutaneous coronary interventions (PCI) *vs.* coronary artery bypass grafting (CABG)] based on the findings of CTA. Later, they were given the CT-FFR data and again asked to give their consensus decision on management. The management plan was changed in 36% of patients, with eventual 30% reduction in PCI, and 18% change of vessel for PCI (33), and overall combined change of 44% (73). Among these patients, 12% were reallocated from optimal medical to PCI, which is similar to that of original RIPCORD study which evaluated ICA and invasive FFR (74). Outcomes of CT-FFR have also been evaluated in few studies. In the PLATFORM trial, CT-FFR obviated need for ICA in 61% patients with chest pain and CAD who would have been referred for ICA based on results of CTA alone. Further, a CT-FFR-guided approach significantly lowered the rate of ICA demonstrating normal or non-obstructive CAD (12% *vs.* 73%) in those intended for ICA (75). A CT-FFR based strategy may also improve quality of life

Table 2 Diagnostic performance of CT-FFR in various studies

Studies	Software	Types	Reference standard	Levels	Accuracy (%)	Sensitivity (%)	Specificity (%)	Positive predictive value (%)	Negative predictive value (%)	AUC
Koo <i>et al.</i> (66) (DISCOVER-FLOW)	HeartFlow	Multi-center, prospective	Invasive FFR	Patient	87	93	82	85	91	0.75
Min <i>et al.</i> (67) (DEFACTO)	HeartFlow	Multi-center, prospective	Invasive FFR	Patient	73	90	54	67	84	0.80
Nørgaard <i>et al.</i> (68) (NXT)	HeartFlow	Multi-center, prospective	Invasive FFR	Patient	81	86	79	65	93	0.90
Kim <i>et al.</i> (69)	HearFlow	Multi-center, prospective	Invasive FFR	Patient	77	85	57	83	62	–
Renker <i>et al.</i> (61)	Siemens cFFR	Single center, retrospective	Invasive FFR	Patient	NA	94	84	65	93	0.91
Coenen <i>et al.</i> (62)	Siemens cFFR	Single center, retrospective	Invasive FFR	Patient	75	88	65	65	88	0.83
De Geer <i>et al.</i> (70)	Siemens cFFR	Single center, retrospective	Invasive FFR	Lesion	78	83	76	56	83	NA
Baumann <i>et al.</i> (71)	Metaanalysis	Metaanalysis	Invasive FFR	Patient	83	89	70	69	90	0.87
Wu <i>et al.</i> (72)	Metaanalysis	Metaanalysis	Invasive FFR	Patient	NA	89	76	NA	NA	NA

AUC, area under the curve; CT-FFR, computed tomography-derived fractional flow reserve; NA, not available.

and lower costs. In a study by Hlatky *et al.*, CT-FFR was associated with 30% lower costs and 12% fewer MACE at 1 year compared to ICA and visual guidance (76). Among patients with CT-FFR >0.8 for whom ICA was deferred, no patients experienced MACE within a 12-month follow-up period, supporting feasibility and safety of CT-FFR in the real world (61,73).

However, CT-FFR has several limitations. A recent systematic review found that although the overall accuracy of CT-FFR is 81.9%, high accuracy is observed only at extremes of CT-FFR values. The accuracy is significantly lower in patients with borderline CT-FFR values (i.e., 0.7–0.8) (77). Furthermore, most of the trials examining CT-FFR had a low prevalence of intermediate stenosis (12.8%), implying selection of lower-risk populations who are more likely to benefit from non-invasive imaging compared to invasive FFR (77). Data comparing CT-FFR with other noninvasive tests such as SPECT MPI is limited, with one study showing no additional benefit (75). In addition, CT-FFR has only modest diagnostic performance for the detection of ischemia in non-culprit

lesions in patients with recent ST-elevation myocardial infarction (STEMI), likely related to the smaller vessel volume in these patients than stable angina, with the vessel lumen volume relative to myocardial mass affecting the diagnostic performance of CT-FFR (78). Although some earlier studies showed good reproducibility of CT-FFR, this was not evaluated in the trials mentioned above (79). There is also poor numerical matching between CT-FFR and invasive FFR values, calling into question the threshold value of 0.80 used to determine lesion-specific ischemia with CT-FFR (77). Larger multicenter trials with outcomes data in specific patient populations will be required before widespread acceptance of this technology.

The added costs of CT-FFR may also be prohibitive (up to \$1,500 per case) (80). However, a Category III CPT code was recently approved for CT-FFR which will allow this technology to be tracked by the American Medical Association beginning in January 2018, an important first step towards widespread coverage and reimbursement (81). Another current limitation of CT-FFR is the processing/turnaround time, often several hours when data is

transferred off-site, further challenging the evaluation of acute chest pain in the emergency room (ER) setting, although on-site solutions are currently available in some centers. High image quality is required, especially without motion and misalignment, which needs good scanners and expertise. Although the algorithm was initially limited in patients with calcium, stents and bypass grafts, a recent study found that the accuracy of CT-FFR in patients with high calcium is superior to that of CT alone (82).

Recent studies have shown that CT-FFR can provide additional information on biomechanical forces acting on plaques, such as plaque stress, plaque strain and radius gradient (83), all of which play roles in plaque initiation and progression (84). These CT-FFR derived biomechanical forces also provide superior information in predicting acute coronary syndrome (ACS) than stenosis and high-risk plaque features (AUC, 0.727 *vs.* 0.675 *vs.* 0.673, respectively) and also provides incremental risk stratification tool (85). Lipid-rich plaques with large necrotic core and positive remodeling have been shown to be associated with FFR <0.8, independent of the degree of luminal narrowing. This has been shown to be an independent predictor of ACS. With positive remodeling, the smooth muscles are stretched and possibly unable to dilate further on administration of vasodilators for invasive FFR measurement (63,64).

TAG

Coronary arterial TAG is relatively simple technique of estimating the hemodynamic significance of coronary stenosis from a routine CTA without additional contrast, radiation, change of protocol or complex post-processing. TAG is the gradient of luminal attenuation in Hounsfield units (HU) along the coronary artery and is usually measured along the coronary artery at 5-mm intervals from the ostium to the point where the arterial dimension decreases to <2 mm² (Figure 3). TAG is defined as the HU change per 10 mm of coronary artery and defined as linear regression coefficient between the luminal attenuation and length from ostium in mm. In a small study of 54 patients, a cut-off of -15.1 HU/10 mm is considered to be highly accurate, with sensitivity of 77%, specificity of 74%, PPV of 67% and NPV of 86% to predict FFR <0.8 (86). TAG has higher specificity than CT and adding TAG to CTA improves the specificity of CTA to detect functionally significant FFR (83), with improved AUC of 0.88 compared to 0.81 for TAG alone. TAG can be used in patients with unstable angina, which is a limitation

of CT-FFR (86). However, this technique ideally requires a volume/wide array scanner, such as a 320-detector scanner so that the entire heart is scanned in one heartbeat. With smaller detector scanners, differences in contrast timing for different segments of the coronary arteries result in artefactual attenuation gradients and misregistration artifacts. TAG studies performed on 64–256 slice scanners did not show significant difference from CTA and were inferior to CT-FFR (87). TAG can be performed both at rest and stress with comparable AUC (0.78 and 0.75), but the image quality of stress TAG was lower along with higher radiation due to two acquisitions (88).

Comparison of modalities

An ideal comparison of the efficacy of the above-mentioned modalities will require large, multi-center randomized controlled trials. However, this is lacking and even small-scale comparison studies are limited. Since CT-FFR and CTP are fundamentally different, there is no unifying gold standard invasive test, although invasive FFR is a good surrogate. A small two-center study on 74 patients in which both dynamic CTP and CT-FFR (on-site) were performed on the same patients showed that both the techniques have comparable efficacy (accuracy, 70% both; AUC, 0.78 both; specificity, 68% *vs.* 60%; sensitivity, 73% *vs.* 82%) in the detection of hemodynamically significant stenosis with invasive FFR as gold standard (89). Whereas the combination of CTA and CTP significantly improves the diagnostic performances of either of these two techniques individually (AUC, 0.83 *vs.* 0.78), the combination of CTA and CT-FFR only results in a small, statistically insignificant improvement (AUC, 0.80 *vs.* 0.78) than either of these two techniques individually. A single functional CT variable that integrates data from both CT-MPI and CT-FFR had superior performance than these tests separately (accuracy of 79% *vs.* 70%, individually; AUC, 0.85 *vs.* 0.78, individually), indicating that these tests provide complementary information. A step-wise diagnostic work up of CT-FFR followed by selective use of CTP also had an improved accuracy of 77% than the two tests individually (86). In patients who had CT-FFR values between 0.74 and 0.85 (i.e., intermediate stenosis), the accuracy of CT-FFR alone was 55%, but combined with CTP, the accuracy increased to 77%, indicating improved hemodynamic classification of intermediate stenosis. In addition, the step-wise approach will theoretically avoid CTP in 46% of patients, i.e., 69% of territories (89). Another similar study by Yang *et al.* in

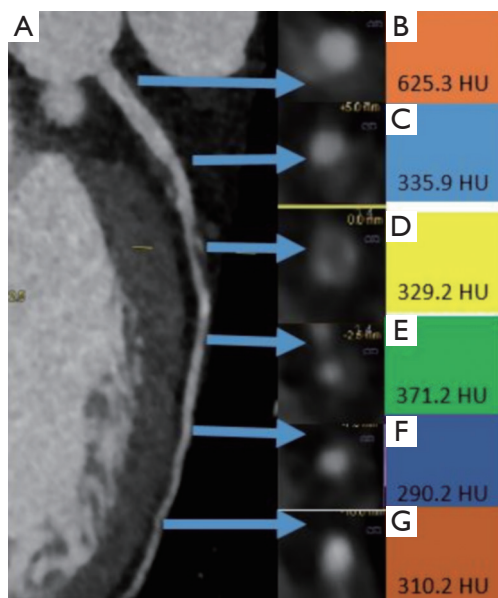


Figure 3 Transluminal attenuation gradient. (A) Left anterior descending coronary artery with non-calcific atherosclerotic plaques; (B-G) axial cross-sectional views at multiple levels are used to measure intraluminal attenuation (HU) at 5-mm intervals. TAG is defined as the HU change per 10 mm of coronary artery and defined as linear regression coefficient between the luminal attenuation and length from ostium in mm. This patient has a TAG of 36, which is considered to be significant. TAG, transluminal attenuation gradient.

72 patients using on-site FFR showed no difference in AUC between CT-FFR and CTP and the diagnostic performance of CTA (AUC, 0.856) was improved by combining it with CT-FFR (AUC, 0.919) or CTP (AUC, 0.913) (90). A meta-analysis showed that CTP and CT-FFR improve the specificity of CCTA for detecting hemodynamically significant stenosis defined by invasive FFR on a per-patient level with pooled specificities of 0.77, 0.72 and 0.43 and PPV of 0.83, 0.70 and 0.56 respectively (91).

A sub-study of NXT study showed that CT-FFR had better correlation with invasive FFR than TAG320, in terms of accuracy (93% vs. 78%), sensitivity (92% vs. 58%), specificity (79% vs. 86%), PPV (65% vs. 65%), NPV (96% vs. 83%), AUC (0.93 vs. 0.72) (87). This is likely due to the differences in principles of each technique. TAG is a surrogate for resting coronary blood flow based on in-vitro observation (87) and is likely influenced by epicardial as well as microvascular resistance; hence, a linear relationship between flow and pressure cannot be assumed (87). This

is not the case with FFR, where assumptions are made for conditions of hyperemia and microvascular resistance. The low sensitivity of TAG in this study may be due to algorithmic errors in luminal contouring causing premature cessation of sampling of HU in the distal vessel, which can cause an artefactual overestimation of TAG, leading it to be less negative and hence a lot of false negatives (87). Another study which compared TAG, CTA, CTP, and integrated TAG + CTA+ CTP found that the accuracy of integrated method was superior than either TAG + CTA, or CTP + CTA, with AUC of 0.91, 0.844, 0.845, respectively in detection of FFR-significant stenosis. While CTA predicted FFR-significant stenosis with sensitivity and specificity of 89%, and 65%, respectively, corresponding values for integrated technique were 88% and 83% (92).

Perspective

It is indeed an exciting time to be a cardiac imager with at least three emerging CT techniques available for the assessment of myocardial ischemia, thus improving the capabilities of CT and moving it closer to a one-stop-shop providing anatomic and functional assessment of CAD. This combination complements the high NPV of CTA with the high specificity and PPV of functional imaging, providing an optimal strategy for guiding appropriate revascularization

Table 3 illustrates the pros and cons of these CT techniques. While CTP requires at least one additional phase of scan resulting in higher radiation dose and contrast, CT-FFR and TAG do not require any protocol modifications, radiation or contrast. The accuracy of these techniques for the detection of hemodynamically significant ischemia has been established, with more evidence available for CTP and FFR than TAG. Each technique appears to be superior to conventional CTA for detection of lesion-specific ischemia. Some studies have directly compared these techniques, but these are limited with small sample sizes. Large randomized trials will be necessary to evaluate their comparative effectiveness. Due to their fundamentally different principles, CT-FFR, CTP and TAG may be useful in different populations. For example, CTP is likely to be of greater value in the evaluation of heavily calcified lesions and coronary stents (93). CTP has shown higher diagnostic accuracy when combined with CTA in patients with heavy calcium (>400) (94). However, CT-FFR is likely to be more useful than CTP in the evaluation of balanced ischemia, since CTP relies on relative hypoperfusion compared

Table 3 Pros and cons of the different CT techniques of myocardial ischemia

Techniques	Pros	Cons
CT perfusion	Hemodynamic significance of stenosis; Effective reclassification of stenotic lesions; More cost-effective than SPECT; Useful in heavy calcium or stent	Not widely available; Advanced skills for performance, post-processing, interpretation; Higher radiation; Larger volume of iodinated contrast; Higher cost than CTA alone; Limited in balanced ischemia
CT-FFR	Hemodynamic significance of stenosis; Effective gatekeeper for ICA; Lower cost and improved outcomes compared to ICA and visual guidance; Biomechanical information on plaques; Effective in balanced ischemia; No additional radiation; No additional contrast	Accuracy lower in borderline values (0.7 to 0.8); Modest performance in non-culprit lesions in recent STEMI; Added cost; Limited availability; Long post-processing time; High image quality required with low motion; Limited in calcium, stents and bypass grafts
TAG	Hemodynamic significance of stenosis; No additional radiation; No additional contrast; No complex post-processing; No additional cost	No outcome data yet; Requires wide array/volume scanner

CT-FFR, computed tomography-derived fractional flow reserve; SPECT, single-photon emission computed tomography; CTA, computed tomography angiogram; ICA, invasive coronary angiogram; STEMI, ST-elevation myocardial infarction; TAG, transluminal attenuation gradient.

to normal myocardium. CT-FFR may be more useful in patients with multi-vessel disease or serial lesions, since it can identify specific ischemic lesions that would benefit from revascularization. There have been outcomes data for CTP and FFR, with studies demonstrating that the addition of these techniques to CTA yields a more effective gatekeeper for selecting patients for cardiac catheterization by reducing the number of false positives, particularly in patients with moderate (50–70%) stenosis. This reduces the prevalence of non-obstructive disease in ICA, limiting ICA for revascularization cases, which results in overall optimization of resources and downstream cost savings.

In spite of all this evidence, significant challenges remain in the widespread adoption of these technologies, which are currently limited to select tertiary care centers. Most of these technologies require state-of-the-art equipment or software, not accessible for all institutions. CTP requires

a good quality scanner and considerable resources have to be invested to establish a dedicated program including advanced protocols and workflow, highly skilled staff, equipment, nursing care and post-processing. Although FFR and TAG do not require additional hardware and can be performed with a routine coronary CTA, CT-FFR performed using HeartFlow requires transfer to off-site center for advanced post-processing and involves additional fee. The on-site reduced order vendor-driven algorithms, are not yet approved and are available only in select institutions. CT-FFR also requires a high-quality CTA with minimal motion. TAG does not require any complex post processing, but it works well only with a wide-array/volume scanner, which is not available in all institutions. With the availability of such possibly competitive technologies which can be performed in different ways in different platforms, it is imperative for the cardiac CT community to take

additional steps to standardize the performance, techniques and interpretation, come up with appropriateness criteria and improve the accessibility of the technique (53).

Conclusions

CT evaluation of myocardial ischemia is now possible with state-of-the-art functional techniques such as CTP, CT-FFR and TAG. Combination of CTA and functional CT provides high negative predictive value as well as high specificity, which enables the accurate detection of ischemia-inducing lesions in patients with intermediate stenosis, and hence select appropriate patients for invasive angiography and revascularization. However, further studies are required for long-term outcomes of these tests and if and how they can replace traditional diagnostic approaches.

Acknowledgements

None.

Footnote

Conflicts of Interest: The authors have no conflicts of interest to declare.

References

- Hamon M, Biondi-Zoccai GG, Malagutti P, et al. Diagnostic performance of multislice spiral computed tomography of coronary arteries as compared with conventional invasive coronary angiography: a meta-analysis. *J Am Coll Cardiol* 2006;48:1896-910.
- Vanhoenacker PK, Heijenbrok-Kal MH, Van Heste R, et al. Diagnostic performance of multidetector CT angiography for assessment of coronary artery disease: meta-analysis. *Radiology* 2007;244:419-28.
- Galperin-Aizenberg M, Cook TS, Hollander JE, et al. Cardiac CT angiography in the emergency department. *AJR Am J Roentgenol* 2015;204:463-74.
- SCOT-HEART investigators. CT coronary angiography in patients with suspected angina due to coronary heart disease (SCOT-HEART): an open-label, parallel-group, multicentre trial. *Lancet* 2015;385:2383-91.
- Lubbers M, Dedic A, Coenen A, et al. Calcium imaging and selective computed tomography angiography in comparison to functional testing for suspected coronary artery disease: the multicentre, randomized CRESCENT trial. *Eur Heart J* 2016;37:1232-43.
- Shaw LJ, Phillips LM, Nagel E, et al. Comparative Effectiveness Trials of Imaging-Guided Strategies in Stable Ischemic Heart Disease. *JACC Cardiovasc Imaging* 2017;10:321-34.
- Moss AJ, Williams MC, Newby DE, et al. The Updated NICE Guidelines: cardiac CT as the first-line test for coronary artery disease. *Curr Cardiovasc Imaging Rep* 2017;10:15.
- McKavanagh P, Lusk L, Ball PA, et al. A comparison of cardiac computerized tomography and exercise stress electrocardiogram test for the investigation of stable chest pain: the clinical results of the CAPP randomized prospective trial. *Eur Heart J Cardiovasc Imaging* 2015;16:441-8.
- Meijboom WB, Van Mieghem CA, van Pelt N, et al. Comprehensive assessment of coronary artery stenoses: computed tomography coronary angiography versus conventional coronary angiography and correlation with fractional flow reserve in patients with stable angina. *J Am Coll Cardiol* 2008;52:636-43.
- Danad I, Szymonikfa J, Twisk JW, et al. Diagnostic performance of cardiac imaging methods to diagnose ischemia-causing coronary artery disease when directly compared with fractional flow reserve as a reference standard: a meta-analysis. *Eur Heart J* 2017;38:991-8.
- Patel MR, Peterson ED, Dai D, et al. Low diagnostic yield of elective coronary angiography. *N Engl J Med* 2010;362:886-95.
- Patel MR, Dai D, Hernandez AF, et al. Prevalence and predictors of non-obstructive coronary artery disease identified with coronary angiography in contemporary clinical practice. *Am Heart J* 2014;167:846-52.
- Tonino PA, De Bruyne B, Pijls NH, et al. Fractional flow reserve versus angiography for guiding percutaneous coronary intervention. *N Engl J Med* 2009;360:213-24.
- De Bruyne B, Fearon WF, Pijls NH, et al. Fractional flow reserve-guided PCI for stable coronary artery disease. *N Engl J Med* 2014;371:1208-17.
- Kang DK, Schoepf UJ, Bastarrika G, et al. Dual-energy computed tomography for integrative imaging of coronary artery disease: principles and clinical applications. *Semin Ultrasound CT MR* 2010;31:276-91.
- Varga-Szemes A, Meinerl FG, De Cecco CN, et al. CT myocardial perfusion imaging. *AJR Am J Roentgenol* 2015;204:487-97.
- Rodríguez-Granillo GA, Carrascosa P, Cipriano S, et al. Beam hardening artifact reduction using dual energy

- computed tomography: implications for myocardial perfusion studies. *Cardiovasc Diagn Ther* 2015;5:79-85.
18. Rodríguez-Granillo GA, Rosales MA, Degrossi E, et al. Signal density of left ventricular myocardial segments and impact of beam hardening artifact: implications for myocardial perfusion assessment by multidetector CT coronary angiography. *Int J Cardiovasc Imaging* 2010;26:345-54.
 19. Bauer RW, Kerl JM, Fischer N, et al. Dual-energy CT for the assessment of chronic myocardial infarction in patients with chronic coronary artery disease: comparison with 3-T MRI. *AJR Am J Roentgenol* 2010;195:639-46.
 20. Ko SM, Song MG, Chee HK, et al. Diagnostic performance of dual-energy CT stress myocardial perfusion imaging: direct comparison with cardiovascular MRI. *AJR Am J Roentgenol* 2014;203:W605-13.
 21. Kurata A, Mochizuki T, Koyama Y, et al. Myocardial perfusion imaging using adenosine triphosphate stress multi-slice spiral computed tomography: alternative to stress myocardial perfusion scintigraphy. *Circ J* 2005;69:550-7.
 22. George RT, Arbab-Zadeh A, Miller JM, et al. Computed tomography myocardial perfusion imaging with 320-row detector computed tomography accurately detects myocardial ischemia in patients with obstructive coronary artery disease. *Circ Cardiovasc Imaging* 2012;5:333-40.
 23. Blankstein R, Shturman LD, Rogers IS, et al. Adenosine-induced stress myocardial perfusion imaging using dual-source cardiac computed tomography. *J Am Coll Cardiol* 2009;54:1072-84.
 24. Cury RC, Magalhaes TA, Paladino AT, et al. Dipyridamole stress and rest transmural myocardial perfusion ratio evaluation by 64 detector-row computed tomography. *J Cardiovasc Comput Tomogr* 2011;5:443-8.
 25. George RT, Arbab-Zadeh A, Miller JM, et al. Adenosine stress 64 and 256 row detector computed tomography angiography and perfusion imaging: a pilot study evaluating the transmural extent of perfusion abnormalities to predict atherosclerosis causing myocardial ischemia. *Circ Cardiovasc Imaging* 2009;2:174-82.
 26. Cury RC, Magalhaes TA, Borges AC, et al. Dipyridamole stress and rest myocardial perfusion by 64 detector row computed tomography in patients with suspected coronary artery disease. *Am J Cardiol* 2010;106:310-5.
 27. Rochitte CE, George RT, Chen MY, et al. Computed tomography angiography and perfusion to assess coronary artery stenosis causing per-fusion defects by single photon emission computed tomography: the CORE320 study. *Eur Heart J* 2014;35:1120-30.
 28. Nasir A, Ko BS, Leung MC, et al. Diagnostic accuracy of combined coronary angiography and adenosine stress myocardial perfusion imaging using 320-detector computed tomography: pilot study. *Eur Radiol* 2013;23:1812-21.
 29. Osawa K, Miyoshi T, Koyama Y, et al. Additional diagnostic value of first-pass myocardial perfusion imaging without stress when combined with 64-row detector coronary CT angiography in patients with coronary artery disease. *Heart* 2014;100:1008-15.
 30. Kachenoura N, Gaspar T, Lodato JA, et al. Combined assessment of coronary anatomy and myocardial perfusion using multidetector computed tomography for the evaluation of coronary artery disease. *Am J Cardiol* 2009;103:1487-94.
 31. Rocha-Filho JA, Blankstein R, Shturman LD, et al. Incremental value of adenosine-induced stress myocardial perfusion imaging with dual-source CT at cardiac CT angiography. *Radiology* 2010;254:410-9.
 32. Bettencourt N, Chiribiri A, Schuster A, et al. Direct comparison of cardiac magnetic resonance and multidetector computed tomography stress-rest perfusion imaging for detection of coronary artery disease. *J Am Coll Cardiol* 2013;61:1099-107.
 33. Ko BS, Cameron JD, Meredith IT, et al. Computed tomography stress myocardial perfusion imaging in patients considered for revascularization: a comparison with fractional flow reserve. *Eur Heart J* 2012;33:67-77.
 34. Feuchtner G, Goetti R, Plass A, et al. Adenosine stress high-pitch 128-slice dual-source myocardial computed tomography perfusion for imaging of reversible myocardial ischemia: comparison with magnetic resonance imaging. *Circ Cardiovasc Imaging* 2011;4:540-9.
 35. Weininger M, Schoepf UJ, Ramachandra A, et al. Adenosine-stress dynamic real-time myocardial perfusion CT and adenosine-stress first-pass dual-energy myocardial perfusion CT for the assessment of acute chest pain: initial results. *Eur J Radiol* 2012;81:3703-10.
 36. Ho KT, Chua KC, Klotz E, et al. Stress and rest dynamic myocardial perfusion imaging by evaluation of complete time-attenuation curves with dual-source CT. *JACC Cardiovasc Imaging* 2010;3:811-20.
 37. Wang Y, Qin L, Shi X, et al. Adenosine-stress dynamic myocardial perfusion imaging with second-generation dual-source CT: comparison with conventional catheter coronary angiography and SPECT nuclear myocardial perfusion imaging. *AJR Am J Roentgenol* 2012;198:521-9.

38. Greif M, von Ziegler F, Bamberg F, et al. CT stress perfusion imaging for detection of haemodynamically relevant coronary stenosis as defined by FFR. *Heart* 2013;99:1004-11.
39. Rossi A, Dharampal A, Wragg A, et al. Diagnostic performance of hyperaemic myocardial blood flow index obtained by dynamic computed tomography: does it predict functionally significant coronary lesions? *Eur Heart J Cardiovasc Imaging* 2014;15:85-94.
40. Huber AM, Leber V, Gramer BM, et al. Myocardium: dynamic versus single-shot CT perfusion imaging. *Radiology* 2013;269:378-86.
41. Bamberg F, Marcus RP, Becker A, et al. Dynamic myocardial CT perfusion imaging for evaluation of myocardial ischemia as determined by MR imaging. *JACC Cardiovasc Imaging* 2014;7:267-77.
42. Bastarrika G, Ramos-Duran L, Rosenblum MA, et al. Adenosine-stress dynamic myocardial CT perfusion imaging: initial clinical experience. *Invest Radiol* 2010;45:306-13.
43. Meinel FG, De Cecco CN, Schoepf UJ, et al. First-arterial-pass dual-energy CT for assessment of myocardial blood supply: do we need rest, stress, and delayed acquisition? Comparison with SPECT. *Radiology* 2014;270:708-16.
44. Ruzsics B, Schwarz F, Schoepf UJ, et al. Comparison of dual-energy computed tomography of the heart with single photon emission computed tomography for assessment of coronary artery stenosis and of the myocardial blood supply. *Am J Cardiol* 2009;104:318-26.
45. Carrascosa PM, Deviggiano A, Capunay C, et al. Incremental value of myocardial perfusion overcoronary angiography by spectral computed tomography in patients with intermediate to high likelihood of coronary artery disease. *Eur J Radiol* 2015;84:637-42.
46. Kido T, Watanabe K, Saeki H, et al. Adenosine triphosphate stress dual source computed tomography to identify myocardial ischemia: comparison with invasive coronary angiography. *Springerplus* 2014;3:75.
47. De Cecco CN, Harris BS, Schoepf UJ, et al. Incremental value of pharmacological stress cardiac dual-energy CT over coronary CT angiography alone for the assessment of coronary artery disease in a high-risk population. *AJR Am J Roentgenol* 2014;203:W70-7.
48. Wang R, Yu W, Wang Y, et al. Incremental value of dual-energy CT to coronary CT angiography for the detection of significant coronary stenosis: comparison with quantitative coronary angiography and single photon emission computed tomography. *Int J Cardiovasc Imaging* 2011;27:647-56.
49. Ko SM, Choi JW, Hwang HK, et al. Diagnostic performance of combined noninvasive anatomic and functional assessment with dual-source CT and adenosine-induced stress dual-energy CT for detection of significant coronary stenosis. *AJR Am J Roentgenol* 2012;198:512-20.
50. Ko SM, Park JH, Hwang HK, et al. Direct comparison of stress- and rest-dual-energy computed tomography for detection of myocardial perfusion defect. *Int J Cardiovasc Imaging* 2014;30:41-53.
51. Kim SM, Chang SA, Shin W, et al. Dual-energy CT perfusion during pharmacologic stress for the assessment of myocardial perfusion defects using a second-generation dual source CT: A comparison with cardiac magnetic resonance imaging. *J Comput Assist Tomogr* 2014;38:44-52.
52. Ko SM, Choi JW, Song MG, et al. Myocardial perfusion imaging using adenosine induced stress dual energy computed tomography of the heart: comparison with cardiac magnetic resonance imaging and conventional coronary angiography. *Eur Radiol* 2011;21:26-35.
53. Pelgrim GJ, Dorrius M, Xie X, et al. The dream of a one-stop-shop: Meta-analysis on myocardial perfusion CT. *Eur J Radiol* 2015;84:2411-20.
54. Takx RA, Blomberg BA, El Aidi H, et al. Diagnostic accuracy of stress myocardial perfusion imaging compared to invasive coronary angiography with fractional flow reserve meta-analysis. *Circ Cardiovasc Imaging* 2015;8(1).
55. Feger S, Rief M, Zimmermann E, et al. Patient satisfaction with coronary CT angiography, myocardial CT perfusion, myocardial perfusion MRI, SPECT myocardial perfusion imaging and conventional coronary angiography. *Eur Radiol* 2015;25:2115-24.
56. Lee DS, Husain M, Wang X, et al. Cardiovascular outcomes after pharmacologic stress myocardial perfusion imaging. *Am Heart J* 2016;174:138-46.
57. Meinel FG, Pugliese F, Schoepf UJ, et al. Prognostic value of stress dynamic myocardial perfusion CT in a multicenter population with known or suspected coronary artery disease. *AJR Am J Roentgenol* 2017;208:761-9.
58. van Rosendael AR, Dimitriu-Leen AC, de Graaf MA, et al. Impact of computed tomography myocardial perfusion following computed tomography coronary angiography on downstream referral for invasive coronary angiography, revascularization and outcome at 12 months. *Eur Heart J Cardiovasc Imaging* 2017;18:969-77.
59. Meyer M, Nance JW Jr, Schoepf UJ, et al. Cost-

- effectiveness of substituting dual-energy CT for SPECT in the assessment of myocardial perfusion for the workup of coronary artery disease. *Eur J Radiol* 2012;81:3719-25.
60. Rossi A, Merkus D, Klotz E, et al. Stress myocardial perfusion: imaging with multidetector CT. *Radiology* 2014;270:25-46.
 61. Renker M, Schoepf UJ, Wang R, et al. Comparison of diagnostic value of a novel noninvasive coronary computed tomography angiography method versus standard coronary angiography for assessing fractional flow reserve. *Am J Cardiol* 2014;114:1303-8.
 62. Coenen A, Lubbers MM, Kurata A, et al. Fractional Flow Reserve Computed from Noninvasive CT Angiography Data: Diagnostic Performance of an On-Site Clinician-operated Computational Fluid Dynamics Algorithm. *Radiology* 2015;274:674-83.
 63. Narula J, Nakano M, Virmani R, et al. Histopathologic characteristics of atherosclerotic coronary disease and implications of the findings for the invasive and non-invasive detection of vulnerable plaques. *J Am Coll Cardiol* 2013;61:1041-51.
 64. Ahmadi A, Stone GW, Leipsic J, et al. Association of Coronary Stenosis and Plaque Morphology with Fractional Flow Reserve and Outcomes. *JAMA Cardiol* 2016;1:350-7.
 65. Nørgaard BL, Hjort J, Gaur S, et al. Clinical use of Coronary CTA-derived FFR for decision making in stable CAD. *JACC Cardiovasc Imaging* 2017;10:541-50.
 66. Koo BK, Erglis A, Doh JH, et al. Diagnosis of ischemia-causing coronary stenoses by noninvasive fractional flow reserve computed from coronary computed tomographic angiograms. Results from the prospective multicenter DISCOVER-FLOW (Diagnosis of Ischemia-Causing Stenoses Obtained Via Noninvasive Fractional Flow Reserve) study. *J Am Coll Cardiol* 2011;58:1989-97.
 67. Min JK, Leipsic J, Pencina MJ, et al. Diagnostic accuracy of fractional flow reserve from anatomic CT angiography. *JAMA* 2012;308:1237-45.
 68. Nørgaard BL, Leipsic J, Gaur S, et al. Diagnostic performance of non invasive fractional flow reserve derived from coronary computed tomography angiography in suspected coronary artery disease: the NXT trial (Analysis of coronary blood flow using CT angiography: Next steps). *J Am Coll Cardiol* 2014;63:1145-55.
 69. Kim KH, Doh JH, Koo BK, et al. A novel noninvasive technology for treatment planning using virtual coronary stenting and computed tomography derived computed fractional flow reserve. *JACC Cardiovasc Interv* 2014;7:72-8.
 70. De Geer J, Sandstedt M, Björkholm A, et al. soft based on-site estimation of fractional flow reserve using standard coronary CT angiography data. *Acta Radiol* 2016;57:1186-92.
 71. Baumann S, Renker M, Hetjens S, et al. Comparison of coronary computed tomography angiography-derived vs invasive fractional flow reserve assessment: Meta-analysis with subgroup evaluation of intermediate stenosis. *Acad Radiol* 2016;23:1402-11.
 72. Wu W, Pan DR, Foin N, et al. Noninvasive fractional flow reserve derived from coronary computed tomography angiography for identification of ischemic lesions: a systematic review and meta-analysis. *Sci Rep* 2016;6:29409.
 73. Curzen NP, Nolan J, Zaman AG, et al. Does the routine availability of CT-Derived FFR influence management of Patients With Stable Chest Pain Compared to CT Angiography Alone?: The FFRCT RIPCORD Study. *JACC Cardiovasc Imaging* 2016;9:1188-94.
 74. Curzen N, Rana O, Nicholas Z, et al. Does routine pressure wire assessment influence management strategy at coronary angiography for diagnosis of chest pain?: the RIPCORD study. *Circ Cardiovasc Interv* 2014;7:248-55.
 75. Douglas PS, Pontone G, Hlatky MA, et al. Clinical outcomes of fractional flow reserve by computed tomographic angiography-guided diagnostic strategies vs usual care in patients with suspected coronary artery disease: The prospective longitudinal trial of FFRCT: outcome and resource impacts study. *Eur Heart J* 2015;36:3359-67.
 76. Hlatky MA, Saxena A, Koo BK, et al. Projected costs and consequences of computed tomography-determined fractional flow reserve. *Clin Cardiol* 2013;36:743-8.
 77. Cook CM, Petraco R, Shun-Shin MJ, et al. Diagnostic accuracy of computed tomography-derived fractional flow reserve: A systematic review. *JAMA Cardiol* 2017;2:803-10.
 78. Gaur S, Taylor CA, Jensen JM, et al. FFR derived from coronary CT angiography in non-culprit lesions of patients with recent STEMI. *JACC Cardiovasc Imaging* 2017;10:424-33.
 79. Gaur S, Bezerra HG, Lassen JF, et al. Fractional flow reserve derived from coronary CT angiography: variation of repeated analysis. *J Cardiovasc Comput Tomogr* 2014;8:307-14.
 80. Shaw LJ, Nicol E. Lesion-specific ischemia with noninvasive computed tomographic angiography. Superior to conventional stress testing? *JAMA Cardiol* 2017;2:717-9.

81. CPT® Category III Codes Code Descriptors. Available online: <https://www.ama-assn.org/sites/default/files/media-browser/public/cpt/cpt-category3-codes-descriptors.pdf>
82. Nørgaard BL, Gaur S, Leipsic J, et al. Influence of coronary calcification on the diagnostic performance of CT angiography derived FFR in coronary artery disease. *JACC Cardiovasc Imaging* 2015;8:1045-55.
83. Nørgaard BL, Leipsic J, Koo BK, et al. Coronary computed tomography angiography derived fractional flow reserve and plaque stress. *Curr Cardiovasc Imaging Rep* 2016;9:2.
84. Choi G, Lee JM, Kim HJ, et al. Coronary artery axial plaque stress and its relationship with lesion geometry: Application of computational fluid dynamics to coronary CT angiography. *JACC Cardiovasc Imaging* 2015;8:1156-66.
85. EMERALD: FFRCT accurately predicts which plaques cause ACS. Available online: <https://www.healio.com/cardiac-vascular-intervention/imaging/news/online/%7Bac33727b-6b0d-4555-84af-8d8b7c36dcc3%7D/emerald-ffrct-accurately-predicts-which-plaques-cause-ac>
86. Wong DT, Ko BS, Cameron JD, et al. Transluminal attenuation gradient in coronary computed tomography angiography is a novel noninvasive approach to the identification of functionally significant coronary artery stenosis: a comparison with fractional flow reserve. *J Am Coll Cardiol* 2013;61:1271-9.
87. Ko BS, Wong DT, Nørgaard BL, et al. Diagnostic performance of transluminal attenuation gradient and noninvasive fractional flow reserve derived from 320-detector row CT angiography to diagnose hemodynamically significant coronary stenosis: An NXT substudy. *Radiology* 2016;279:75-83.
88. Ko BS, Seneviratne S, Cameron JD, et al. Rest and stress transluminal attenuation gradient and contrast opacification difference for detection of hemodynamically significant stenoses in patients with suspected coronary artery disease. *Int J Cardiovasc Imaging* 2016;32:1131-41.
89. Coenen A, Rossi A, Lubbers MM, et al. Integrating CT myocardial perfusion and CT-FFR in the work up of coronary artery disease. *JACC Cardiovasc Imaging* 2017;10:760-70.
90. Yang DH, Kim YH, Roh JH, et al. Diagnostic performance of on-site CT-derived fractional flow reserve versus CT perfusion. *Eur Heart J Cardiovasc Imaging* 2017;18:432-40.
91. Gonzalez JA, Lipinski MJ, Flors L, et al. Meta-analysis of diagnostic performance of coronary computed tomography angiography, computed tomography perfusion, and computed tomography-fractional flow reserve in functional myocardial ischemia assessment versus invasive fractional flow reserve. *Am J Cardiol* 2015;116:1469-78.
92. Wong DT, Ko BS, Cameron JD, et al. Comparison of diagnostic accuracy of combined assessment using adenosine stress CT perfusion computed tomography angiography (CTA) with transluminal attenuation gradient (TAG 320) + CTA against invasive fractional flow reserve (FFR). *J Am Coll Cardiol* 2014;63:1904-12.
93. Arbab-Zadeh A, Miller JM, Rochitte CE, et al. Diagnostic accuracy of computed tomography coronary angiography according to pre-test probability of coronary artery disease and severity of coronary arterial calcification. The CORE-64 (Coronary Artery Evaluation Using 64-Row Multidetector Computed Tomography Angiography) International Multicenter Study. *J Am Coll Cardiol* 2012;59:379-87.
94. Sharma RK, Arbab-Zadeh A, Kishi S, et al. Incremental diagnostic accuracy of computed tomography myocardial perfusion imaging over coronary angiography stratified by pre-test probability of coronary artery disease and severity of coronary artery calcification: The CORE320 study. *Int J Cardiol* 2015;201:570-7.

Cite this article as: Rajiah P, Maroules CD. Myocardial ischemia testing with computed tomography: emerging strategies. *Cardiovasc Diagn Ther* 2017;7(5):475-488. doi: 10.21037/cdt.2017.09.06